Proceedings of the 10th International Conference on Civil Structural and Transportation Engineering (ICCSTE 2025)
July, 2025 | Imperial College London Conference Center, London, United Kingdom
Paper No. 271
DOI: 10.11159/iccste25.271

Monitoring Of Temperature-Induced Deformations in High Mountain Huts

Yunlu Bai[1], Francesco Calvetti[1]
[1] Politecnico di Milano, Dept. Architecture, Built Environment and Construction Engineering
P. zza L. da Vinci 32, Milano Italy
yunlu.bai@polimi.it; francesco.calvetti@polimi.it

Abstract – Global warming is affecting a lot of human activities and has a relevant environmental impact. This is particularly evident in the Alps, where the recorded temperature increases are larger than average. This trend has direct consequences on the stability of high mountain slopes, as it provokes the upward receding of permafrost and triggers a series of rockfall events. Although it is difficult to pinpoint the direct cause-effect relationship for any recorded event, two general facts emerge: failures are becoming more and more frequent, especially during particularly hot summer seasons; failures tend to concentrate within the altitude range affected by permafrost receding.
In this paper, we discuss the structural monitoring at Capanna Margherita hut (Punta Gnifetti 4554m a.s.l., Monte Rosa massif), which is the highest mountain hut in the Alps and Europe in general. Geomechanical monitoring was activated there in 2023 and it is now complemented by the installation of sensors on the hut structure in 2024. A full set of data is continuously being recorded, including inclinometric, thermometric and accelerometric data. The paper analysis is based on the data recorded by the sensors and the air temperature at Capanna Margherita hut, including the relationship between the temperatures and displacements, and the dynamic characteristics of structural vibrations.

***Keywords*:** High alps; Permafrost; In-situ testing; Structural monitoring; Vibration analysis

1. Introduction

Air temperature observations across the European Alps, Asia and North America show that warming recently occurred at a rate of 0.3±0.2 °C per decade, which is faster than the global warming rate of 0.2±0.1 °C per decade [1]. The permafrost distributed in alpine areas shows a degradation according to several observations [2]. More specifically, wide evidence of steep rock destabilization caused by warming permafrost is clearly emerging [3], [4]. The influence of warming permafrost in the Mont Blanc range is confirmed by the occurrence of statistically frequent rock slope failures of rock faces where the Mean Annual Rock Surface Temperature (MARST) ranges between -2 °C and 0 °C [5].

Fig 1: Capanna Margherita (4554 m a.s.l.)

In this context, it is fundamental to assess the current and future risk scenarios at high altitudes, in particular with reference to sites with structures (typically mountain huts) and infrastructures. This research is in particular devoted to the modelling of the rock mass of Punta Gnifetti-Signalkuppe (Monte Rosa group) and the effects of permafrost degradation on the stability of Capanna Margherita, which belongs to the Italian Alpine Club. Capanna Margherita is located just on top of Punta Gnifetti at 4554 meters a.s.l. and it is the highest hut, and building in general, in Europe (Fig 1).

The monitoring project at Capanna Margherita started in September 2023. The installation details and the analysis of the first set of recorded geomechanical data have been presented by Bai and Calvetti [6]. This paper introduces the analysis of the monitoring data recorded by 3 additional sensors installed in 2024 inside the hut.

2. In-situ campaign

An insitu measurement campaign has been ongoing at Capanna Margherita since October 2023. In particular, two multi-parametric geotechnical monitoring systems (DMS columns) were installed in boreholes. Considering the climate-driven nature of potential failures, a full set of data is continuously being recorded by these devices, including inclinometric, extensometric, piezometric, thermometric and accelerometric data. The DMS system is completed by a control unit that records the data at prescribed intervals and sends them to a dedicated server via a GSM modem.

2.1 Structural monitoring

To provide additional data, three measurement modules (inclinometer, accelerometer, thermometer) belonging to the same DMS family were installed in 2024 inside Capanna Margherita (Fig 2, Fig 3). Module 3 was installed on July 25th on a vertical strut that rests on rock (see Fig 10) and supports the balcony. The strut is located in a small shelter below the balcony itself, close to the control unit. Modules 4 and 5 were installed on October 24th on two beams at the ground floor ceiling of the structure, respectively in the corridor at the entrance of the winter part of the hut and in the dining room. It is worth noting that the hut was open until September 6th, and since then, only the winter part has been accessible. However, in general, no people are visiting the hut from the end of October until March/April.

Fig 2: Structural modules: a) module 3; b) module 4; c) module 5.

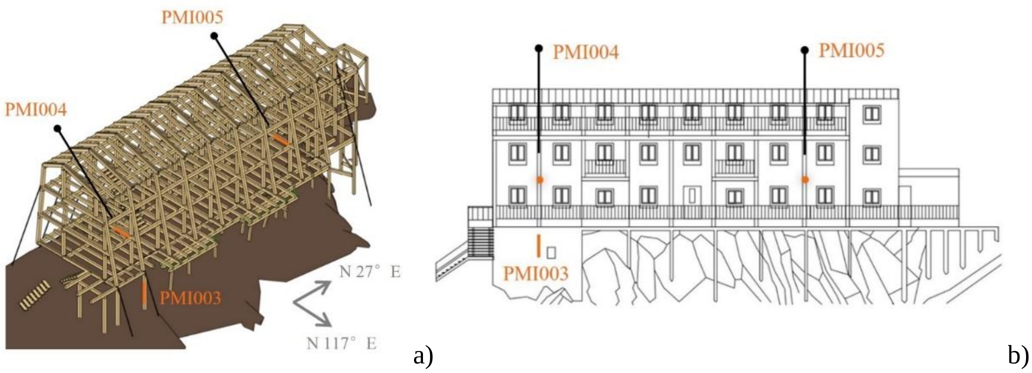

Fig 3: Sensors' arrangement in Capanna Margherita hut. a) 3D sketch of the hut structure; b) front view.

3. Recorded data

In this chapter, we describe the data recorded by the structural modules, focusing on the evolution of temperature and displacements and their relationship. External air temperature, available from the weather station at Capanna Margherita, is also considered in the analysis. It is worth noting that displacements are actually evaluated from inclinometer data, and they correspond to the differential displacement between the ends of each module, assuming a 1 m length in the vertical direction. In order to show results in a meaningful way, displacements are projected along directions N 27°E and N 117°E, which correspond to the longitudinal and transversal axis of the hut (see Fig 3a). In the following, these components will be referred to as d^{27} and d^{117}.

3.1 Mid-term evolution

We first describe the trend of data from module 3 in the span of time between 2024/07/25 and 2024/12/07, which is labelled "mid-term evolution" in that it covers approximately the early-summer to late-autumn period (Fig 4). Information corresponding to the coloured time ranges is interpreted in § 4.1.

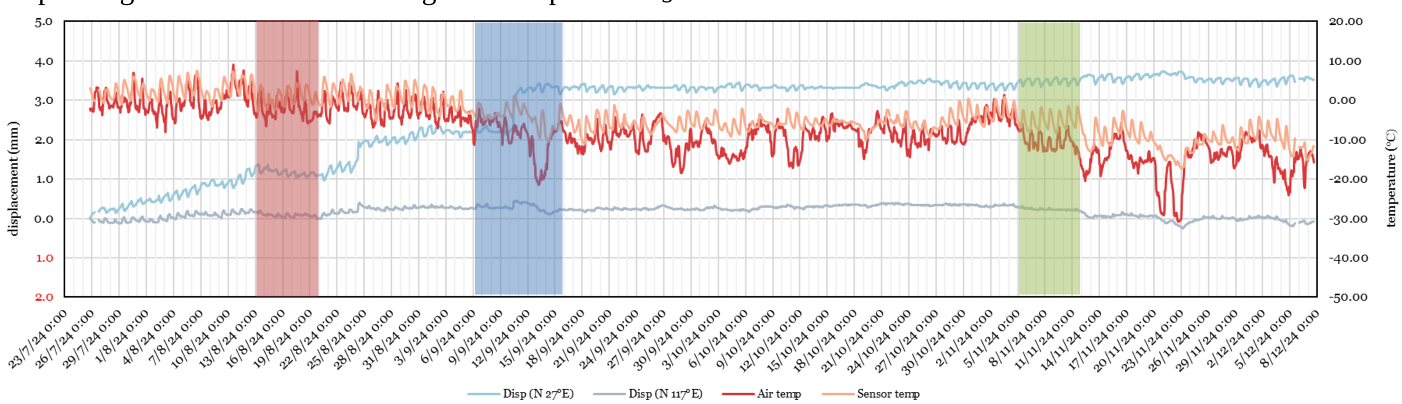

Fig 4: Displacement and temperature recorded in Module 3 and the air temperature at Capanna Margherita hut.

Temperature follows a daily cyclic pattern, oscillating around 0°C (mainly between +7 and –3 °C) until September 6th. After that date, temperatures remain below zero, most of the time between 0 and –10 °C, with a few periods of extremely low temperature (between -20 and –30°C). A more detailed analysis of the temperature trend is given in § 3.2.

Displacements exhibit a cyclic daily trend, as well, which is superimposed to progressive accumulation (non-reversibility relative to thermal cycles). In particular, on two occasions (August 24 between 7 AM and 8 AM and September 10 between 10 AM and 11 AM), sudden increases in displacement were observed, followed by rapid stabilization. The second event occurred when temperatures first dropped significantly. This point will be further analysed in § 4.1 and § 4.2.

3.2 Short-term evolution

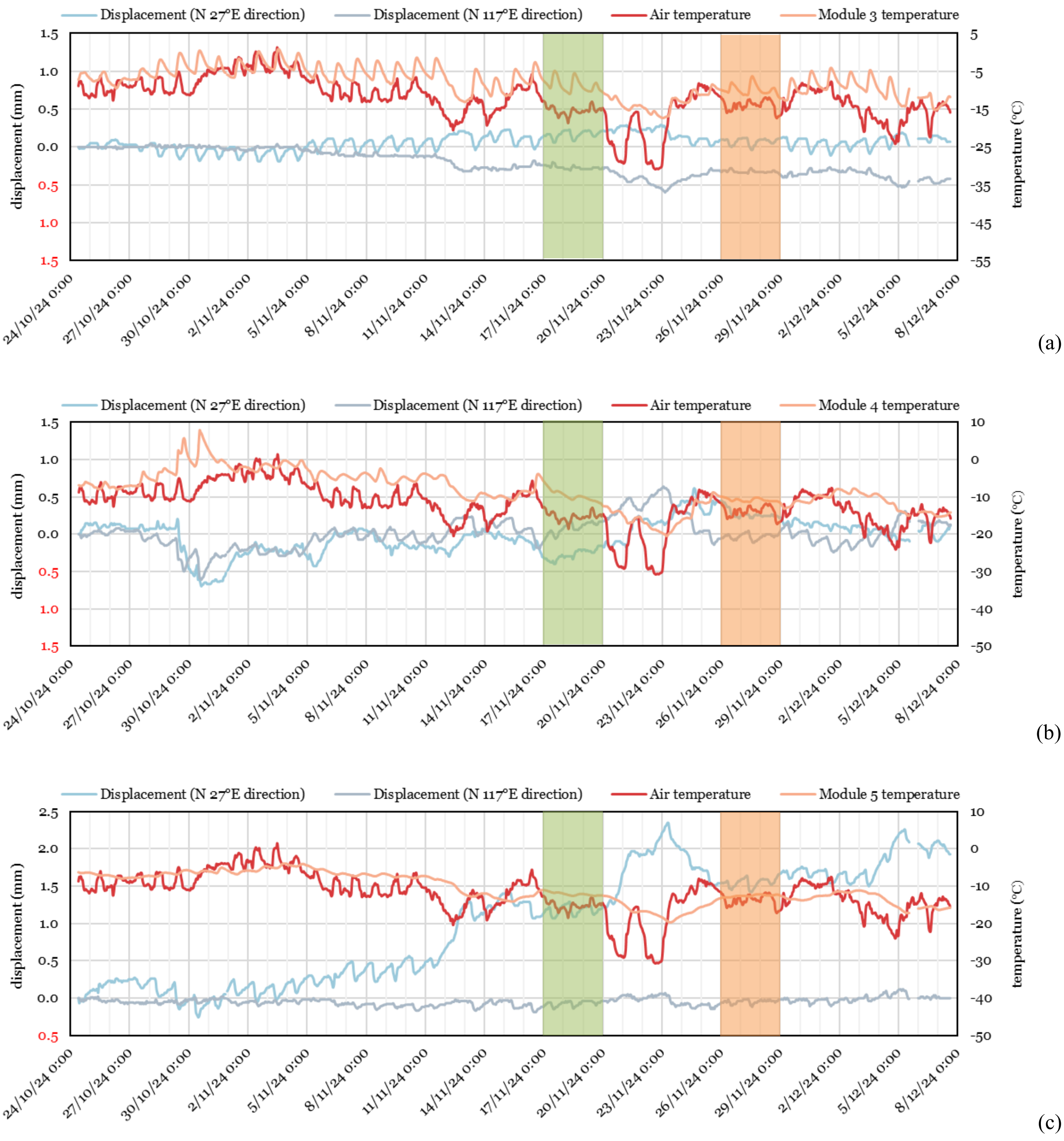

Fig 5: Air temperature, displacements and module temperature. a) module 3; b) module 4; c) module 5.

From October 24th, the data from modules 4 and 5 are available. They are described qualitatively in this paragraph and referred to as “short-term evolution”, which covers the middle portion of Autumn (Fig 5). Information corresponding to the coloured time ranges is interpreted in § 4.1.

With reference to the data plotted in Fig 5 a few general qualitative comments can be drawn. Some of them are general, some are module-specific.

First of all, the temperature recorded by the sensors generally follows the evolution of external air temperature. All temperature trends are characterised by small, more or less marked, daily oscillations and longer periods bigger variations of the daily average. Daily oscillations are more evident in sensor temperature than in external air temperature. This is most probably due to the effect of solar radiation on the dark copper surface of the hut (see Fig 1) with consequent heat transfer to the inside. It is worth noting that the size of the rooms where the sensors are located is approximately 10, 20 and 120 m^3 for sensors 3, 4 and 5, respectively. Moreover, the room where sensor 3 is located is not insulated. This explains why sensor 3 records the larger daily oscillations, which are, on the contrary, barely visible for sensor 5.

Furthermore, daily oscillations of air temperature are almost immediately transferred to sensor temperature oscillations; on the contrary, larger variations of the average air temperature that occur over several days trigger a delayed and smoothened change in sensor temperatures.

The evolution of displacements is similar to what is observed in the longer period for sensor 3 (see § 3.1) and is characterised by a cyclic daily trend which is superimposed to progressive accumulation (non-reversibility relative to thermal cycles). This point will be further analysed in § 4.1

4. Data analysis

4.1 Displacement evolution

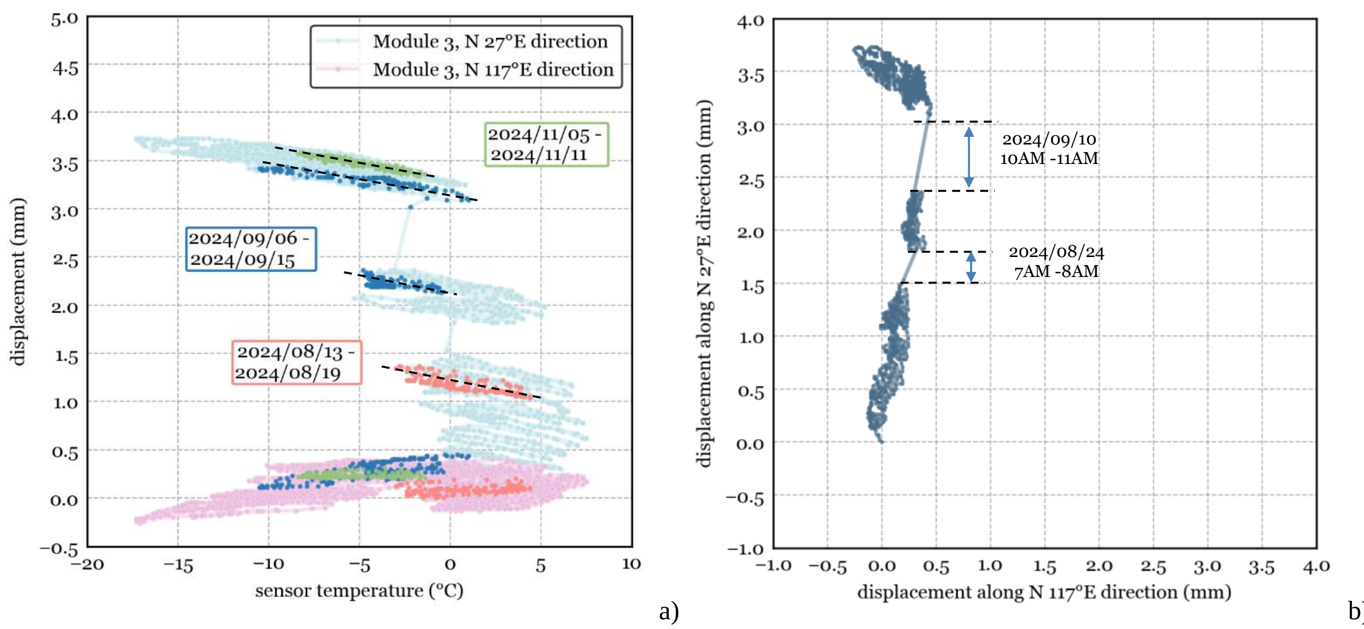

Fig 6: Module 3: a) displacements vs module temperature; b) displacement trajectory.

Fig 6a shows the mid-term relationship between displacements and sensor temperature (module 3). The plotted data confirm the superimposition of a cyclic behaviour with a progressive accumulation of displacements. In order to interpret the data, the following date ranges are highlighted: 2024/08/13-2024/08/19, 2024/09/06-2024/09/15 and 2024/11/05-2024/11/11 (see Fig 4). The first and third periods are characterised by relatively regular daily oscillation of both the sensor temperature and displacement; the central one spans across the rapid displacement increment that occurred on 2024/09/10. First of all, it is worth noting that the displacement component d^{27} is predominant with respect to d^{117}. Within each range, the relationship between d^{27} and temperature can be well-fitted by linear interpolations, whose trends are almost parallel. This is true even if, within the central range, the trends before and after 2024/09/10 are separately considered, as it is confirmed by a statistical analysis with Pearson's coefficients close to -1 between sensor temperature and d^{27} (the Pearson's coefficients for d^{117} shows a less evident correlation, probably due to the smaller values of d^{117}). The approximated linear relationships can be expressed incrementally as $\Delta d^{27} \approx 0.03\Delta T$ which describes the thermal induced reversible displacement (black dotted lines in Fig 6a).

In Fig 6b, the two displacement components d^{27} and d^{117} are plotted against each other, which corresponds to visualising the "trajectory" of the monitored item and allows us to detect the direction of the displacement. It's clear that this latter has significantly changed after 2024/09/10, which suggests that an irreversible evolution of the structure/foundation system has occurred. This point will be further analysed in §4.2.

With reference to the short-term analysis, for which all sensor data are available, it is useful to show and discuss the displacement trajectories first. In fact, from Fig 7, it's clear that the behaviour is completely different when comparing the three sensors. Displacements at sensor 5 are clearly oriented parallel to the longitudinal axis of the hut (N27) and are much bigger than those recorded at sensor 3 and 4. Moreover, while the direction of displacements at sensors 5 and 3 is almost constant, it continuously changes for sensor 4.

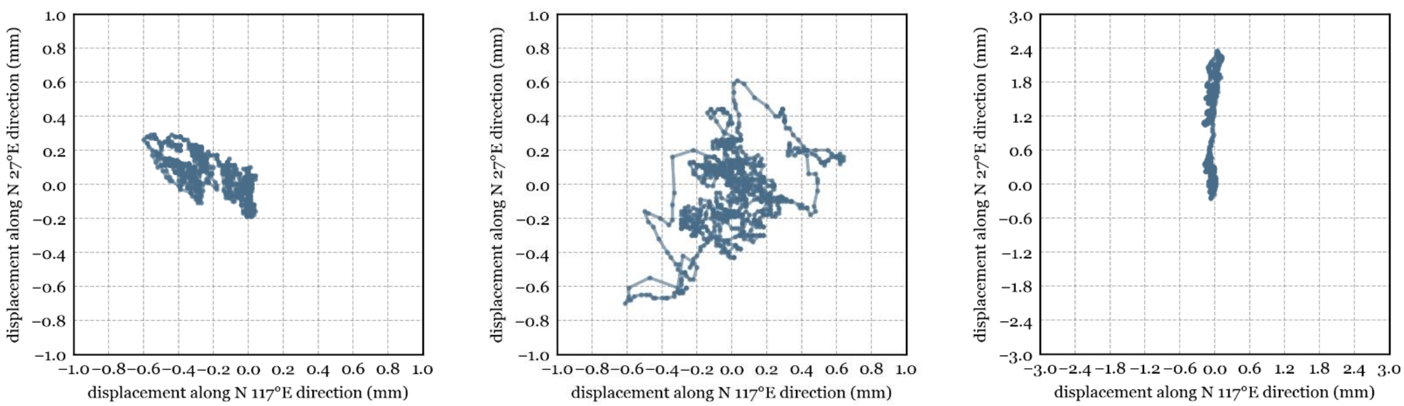

a) b) c)

Fig 7: Displacement trajectory: a) module 3; b) module 4; c) module 5 (period 2024/10/24 - 2024/12/07).

Fig. 8 shows the short-term relationship between displacements and sensor temperature for all modules. Also, with reference to the shorter time interval, the plotted data confirm the superimposition of a cyclic behaviour with a progressive accumulation of displacements. In this case, in order to interpret the data, two date ranges are highlighted: 2024/11/17-2024/11/20 and 2024/11/26-2024/11/29. They correspond to the periods immediately before and after the main variation of air temperature with two cycles between -15 and –30°C (see Fig 5).

First of all, it is worth noting that these data confirm that different responses are recorded by the sensors. In particular, sensor 3 is characterised by the same trend observed for cyclic displacement that was previously highlighted, and the interpolation trend introduced for describing the incremental relationship between temperature and d^{27} is unchanged (dotted lines in Fig 6a and Fig 8a). Moreover, the non reversible effect of the large temperature cycle is evident because two distinct, parallel, lines are required to interpolate the data corresponding to the two considered time windows.

The same qualitative consideration is also valid for displacements recorded at sensors 4 and 5, although the interpretation of data is more complex (especially for sensor 4) due to the continuous rotation of the displacements. In this case (Fig 8b), it is not possible to detect a clear incremental relationship between temperature and the displacements; however, the non-reversible effect of the large temperature cycle is evident. The same considerations are valid for sensor 5 (Fig 8c).

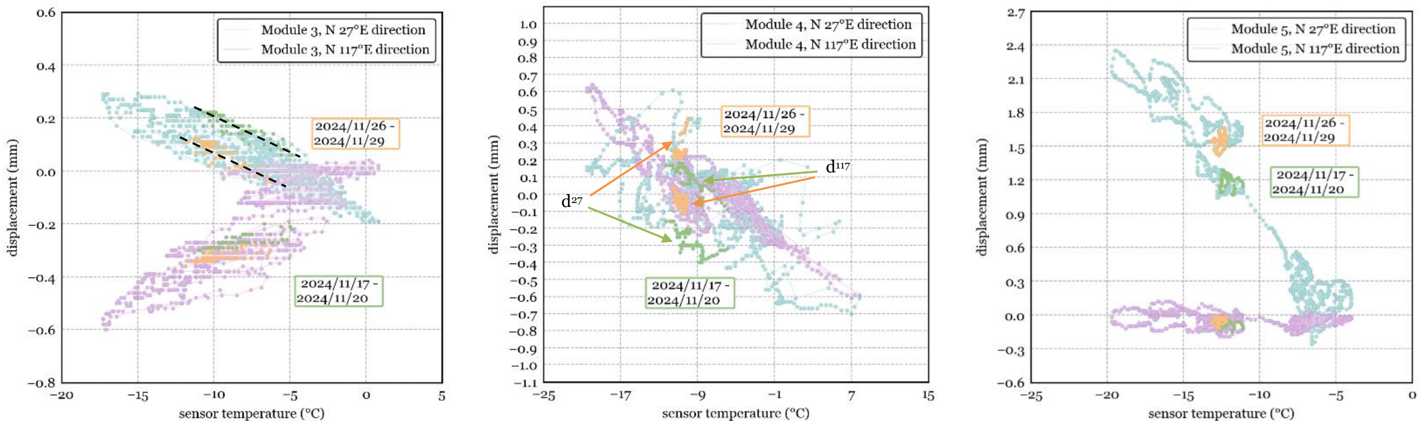

a) b) c)

Fig 8: Displacements vs module temperature: a) module 3; b) module 4; c) module 5 (period 2024/10/24 - 2024/12/07).

4.2 Vibration analysis

The vibrations are recorded by the accelerometer in the sensor when the acceleration exceeds a given threshold in any direction (x, y, and z). Fig 9 summarises the main frequencies in 3 directions of each vibration event recorded in module 3 from 2024/07/25 to 2024/12/07. Since the sampling interval is 4 ms, the maximum frequency that can be captured is 125 Hz. X and y directions correspond to N27 and N117, respectively, while z is vertical.

Before 2024/09/10, the frequency in the z direction, i.e. parallel to the strut axis, was mostly concentrated around 110 Hz. While the frequency in the other two directions, which are perpendicular to the strut axis, is concentrated around 60 Hz (in Fig 9 the corresponding data are almost perfectly superimposed and therefore only one of them is visible). The recorded data, clearly show that the frequency in all three directions has a sudden drop in 2024/09/10, which corresponds to the day when a big displacement increment was recorded in module 3 (Fig 4), as discussed in §3.1 and §4.1. This might indicate that the displacement is linked to a change in structural stiffness because it is unlikely that the mass of the system has changed.

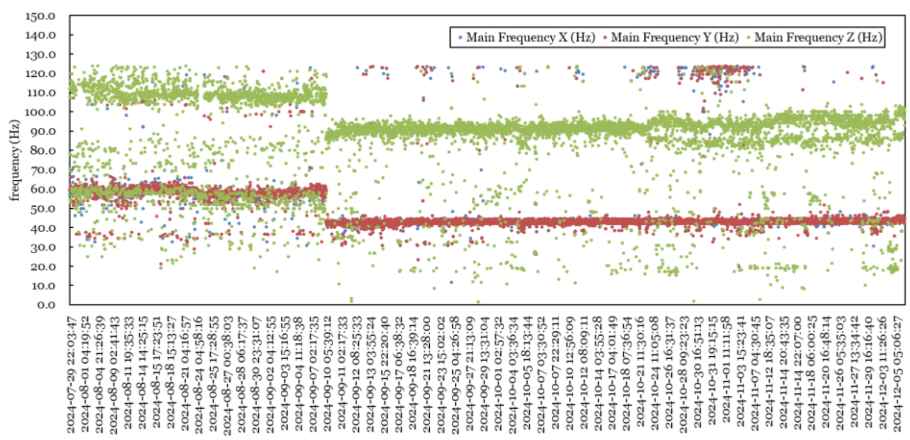

Fig 9: Main frequency of vibrations recorded in Module 3.

In fact, the monitored structural element supports the balcony and is in direct contact with the rock through a simple support constraint (Fig 10). It is therefore possible that the sudden displacement increase is due to some sort of slippage at the strut-rock interface or to a local movement of the support block.

Fig 10: Structure sketch with the position of the monitored strut (module 3, red); typical strut-ground connection at Capanna Margherita.

5. Conclusion

Despite the limited time period (at the moment) covered by the monitoring system, a few observations can already be drawn, as discussed in the text. The main points are reported here.

First of all, it is observed that sensor temperature follows a daily cyclic pattern, influenced by solar radiation and daily oscillations of external air temperature, and reacts to longer term external temperature variations with a delay. Displacements are triggered by thermal variations. They exhibit a drifting cyclic behaviour, characterised by reversible daily oscillations and a progressive accumulation with time. The direction and magnitude of displacements are not uniform across the structure, in that their magnitude and direction are different for the three monitored elements. The magnitude of displacement accumulation is not uniform; albeit this trend is likely associated with relevant variations of temperature, a quantitative interpretation is still missing. As a final remark, the data show a correlation between the occurrence of the most evident displacement increment and a change in: a) the dynamic properties of the affected structural element; b) the direction of its displacements.

Acknowledgements

This research is supported by a China Scholarship Council grant awarded to Yunlu Bai and by the Italian Alpine Club (CAI). The Authors acknowledge the contribution to the installation of the sensors at Capanna Margherita by Fabio Baio, Daniele Bernasconi and helicopter pilot Andrea Romani. The technical support by Luigi Foglino is also gratefully acknowledged.

References

[1] Intergovernmental Panel on Climate Change (IPCC), “Summary for Policymakers,” in Global Warming of 1.5°C: IPCC Special Report on Impacts of Global Warming of 1.5°C above Pre-industrial Levels in Context of Strengthening Response to Climate Change, Sustainable Development, and Efforts to Eradicate Poverty, *Cambridge: Cambridge University Press*, 2022, pp. 1–24.

[2] Intergovernmental Panel on Climate Change (IPCC), The Ocean and Cryosphere in a Changing Climate: Special Report of the Intergovernmental Panel on Climate Change. *Cambridge: Cambridge University Press*, 2022.

[3] S. Gruber, and W. Haeberli, “Permafrost in steep bedrock slopes and its temperature-related destabilization following climate change”, *Journal of Geophysical Research (Earth Surface)*, vol. 112, no. F2, 2007. doi:10.1029/2006JF000547.

[4] L. Ravanel, F. Magnin, and P. Deline, “Impacts of the 2003 and 2015 summer heatwaves on permafrost-affected rock-walls in the Mont Blanc massif”, *Science of The Total Environment*, vol. 609, pp. 132–143, Dec. 2017.

[5] M. Cathala, F. Magnin, L. Ravanel, L. Dorren, N. Zuanon, F. Berger, F. Bourrier and P. Deline., “Mapping release and propagation areas of permafrost-related rock slope failures in the French Alps: A new methodological approach at regional scale”, *Geomorphology*, vol. 448, p. 109032, Mar. 2024.

[6] Y. Bai and F. Calvetti, " Monitoring of Global Warming Effects in High Alps." *In Proceedings of the 9th International Conference on Civil Structural and Transportation Engineering (ICCSTE'24)*, pp. 209/1-8. Avestia, 2024.